VIP Molecular Codes

DOI: 10.1002/ange.200802606

Tunable Molecular Assembly Codes Direct Reaction Pathways**

*Andrew D. Shaller, Wei Wang, Haiyang Gan, and Alexander D. Q. Li**

The physical barrier of a single reaction flask corrals the reaction pathway between a pair of reactants at high concentrations (> 1 mM). In living cells, however, self-organization directs and regulates specific reactions, often at very dilute (ca. nM) concentrations while competing with a myriad of other possible reactants without physical barriers.[1] Nature accomplishes this multifarious task by using dynamic molecular recognition to sort reactive centers according to inherent molecular codes, thus augmenting their effective molarity both efficiently and specifically.[2] Weak secondary forces available for molecular encoding include dispersion forces, coulombic interactions, hydrogen bonding, solvophobic forces, metal–ligand interactions, and π–π stacking interactions.[3] Complex molecular codes can be created from relatively few factors such as size, shape, and charge. The interactive forces are often used simultaneously and synergistically to balance molecular rigidity and flexibility, thereby producing self-sorting effects that control reaction pathways.

Self-assembly by π–π stacking forces, which result from the molecular overlap of π orbitals between planar aromatic systems, has recently attracted much interest.[4] Perylene diimides (PDIs) are particularly interesting because of their efficient assembly,[5] which is often augmented by solvophobic forces, and thus steric groups are often added in either the imide or bay positions to inhibit their strong propensity to self-assemble or ultimately precipitate.[6] However, functionalization of the PDIs with flexible tetraethylene glycol (TEG) chains balances rigidity and flexibility in a wide range of solvents while still allowing dynamic self-assembly (DSA) to manifest its power.[7]

Bay substitutions twist the perylene unit dihedrally out of the plane, with the dihedral angle tunable from 0 to 37°.[8] Herein, we examine DSA between bay-substituted monomers **1**–**4** (Scheme 1a) to broadly establish the role of the dihedral twist angle in molecular encoding.[9] Remarkably, monomers with different twist angles preferentially self-assemble into segregated nanostructures even in the presence of other twisted units, thus revealing their unique molecular encryption (Scheme 1b).

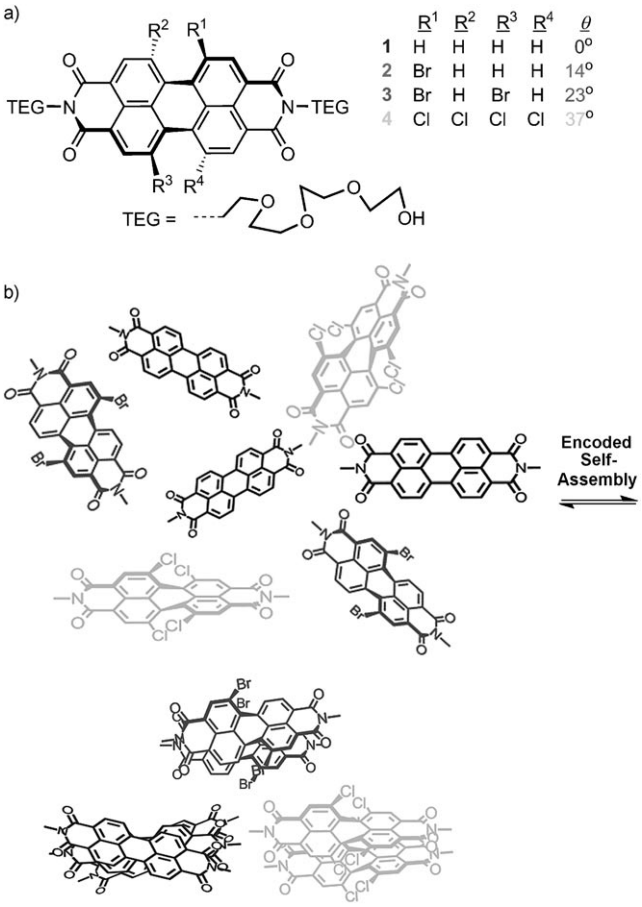

Scheme 1. a) Bay substitutions encode compounds **1**–**4**, twisting them from 0 to 37°. b) Heterogeneous mixtures of encoded PDIs self-sort into homogeneous stacks.

Self-assembly in solution can be readily detected by using complementary spectroscopic methods, especially UV/Vis and NMR spectroscopy.[10] The extent of PDI self-assembly can be monitored by absorbance, as DSA results in a displaced harmonic oscillator that favors excitation to the second vibrational level ($v' = 1$) of the excited state instead of the lowest vibrational level ($v' = 0$). This results in a diagnostic change in the Franck–Condon factors, which is manifested by a dramatic alteration in the ratio of the absorbance vibrational peaks $r_{obs} = A^{0-0}/A^{0-1}$.[9–12]

NMR spectroscopy was used as a complementary technique, and shows the changes in the environment of the aromatic perylene protons, which experience upfield chemical shifts $\Delta\delta_{obs}$ upon assembly as the π-stack ring current increases the shielding of the neighboring protons.[7,9]

[*] A. D. Shaller, Dr. W. Wang, Dr. H. Gan, Prof. A. D. Q. Li
Department of Chemistry
Washington State University
Pullman, WA (USA)
Fax: (+1) 509-335-8867
E-mail: dequan@wsu.edu

[**] We acknowledge support from the National Institute of General Medicine Sciences (Grant GM065306), the Mass Spectrometry Core Laboratories at WSU for discussions concerning MALDI data, and the WSU Center for NMR spectroscopy for assistance with variable temperature NMR studies. A.D.Q.L. is a former Beckman Young Investigator (BYI).

Supporting information for this article is available on the WWW under http://dx.doi.org/10.1002/anie.200802606.

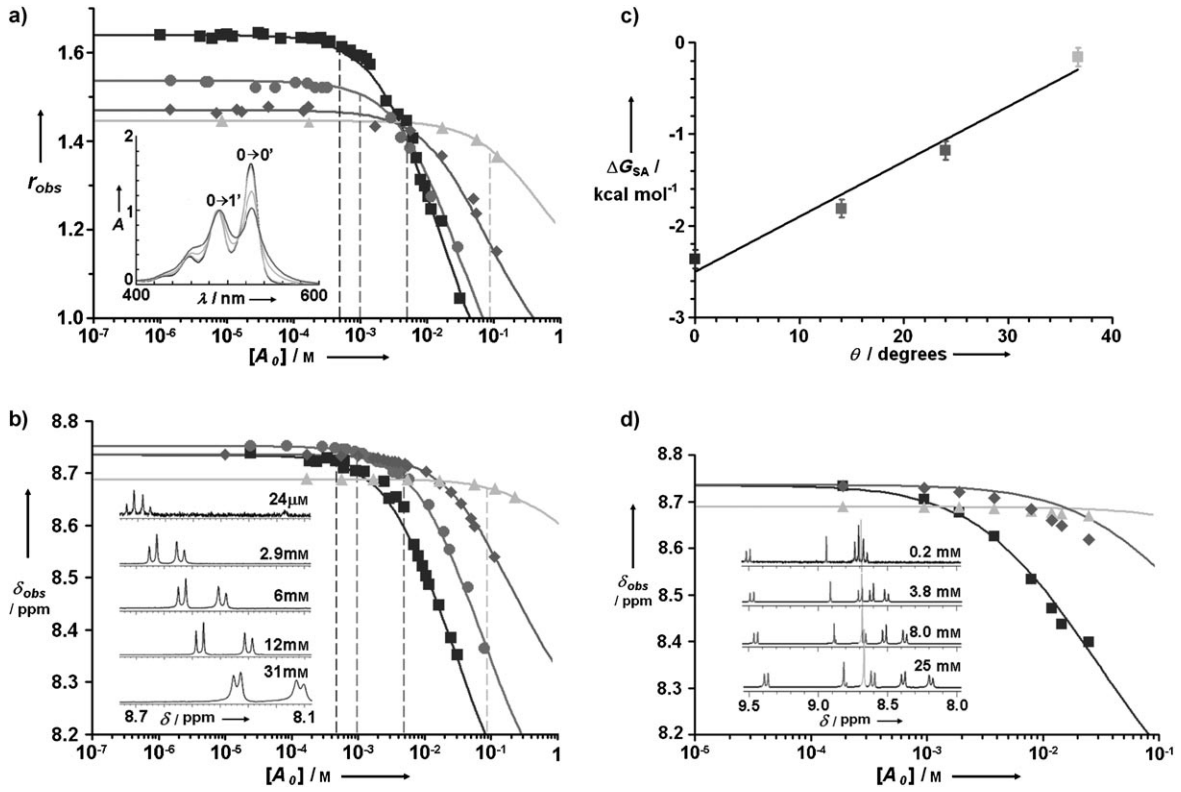

Figure 1. Concentration-dependent a) A^{0-0}/A^{0-1} ratio (r_{obs}) and b) NMR chemical shift (δ_{obs}) for compounds: **1** (■), **2** (●), **3** (◆), and **4** (▲) in $CHCl_3/CDCl_3$ at RT. Values calculated by isodesmic modeling studies are represented by solid lines. Critical assembly concentrations are marked by vertical dashed lines. Typical concentration-dependent spectra for compound **1** are shown as insets. c) Calculated ΔG_{SA} values vary nearly linearly with the dihedral twist angle θ. d) Chemical shifts of the perylene protons for compounds **1**, **3**, and **4** in a 1:1:1 mixture (symbols) compared to the same shifts for separate homogeneous solutions (lines) at equal concentrations. Nearly identical values between the homogeneous and heterogeneous solutions demonstrate almost exclusively independent molecular codes. ^{1}H NMR spectra of the same mixture at four sample concentrations are shown as an inset.

Although all the aromatic protons undergo a change in chemical shift upon stacking, similar non-bay-position protons were compared for consistency between different twisted species.[9]

Both UV/Vis and NMR spectroscopy show that the extent of DSA increases with concentration (Figure 1 a, b); however the monomers **1**–**4** with different twist angles organize at distinct rates and the more highly twisted monomers assemble at increasingly higher concentrations. At low concentrations, the monomers remain mostly free and the observed physical property P_{obs} (r_{obs} or δ_{obs}) shows little change over several orders of magnitude of concentration. Once the concentration reaches the molecular-coded critical concentration dictated by the twist angle, a significant percentage of the monomers form stacked dimers, and P_{obs}, which indicates the collective molecular behavior, begins to change noticeably. Longer stacks form at even higher concentrations, although the rate of change in P_{obs} decreases as the number of assembled units increases. The critical concentration onset covers a broad range (greater than two orders of magnitude), which implies the existence of unique molecular codes that can be exploited to control reaction pathways.

While DSA can be clearly detected by UV/Vis and NMR spectroscopy, determinination of the equilibrium constant (K_{SA}) for indefinite self-association is not trivial, as self-assembled dimers, trimers, and higher stacks typically coexist with the monomer and lead to absorbance ratios and chemical shifts beyond a simplified dimerization model.[7] The value of K_{SA} is determined using the isodesmic equal K model summarized by Martin.[13] In this model, the π-stacking force is assumed to be the same between the ith and $(i+1)$th monomer, and $K_2 = K_3 = \ldots K_\infty = K_{SA}$. The calculated r and δ values, determined from least-squares fitting to the observed values, are plotted as solid lines in Figure 1 a and b.[9] In agreement with Würthner and co-workers,[5b] the free energy for self-assembly ($\Delta G_{SA} = -RT\ln K_{SA}$) exhibits nearly linear dependence on the twist angle (Figure 1 c). Variable solvent composition and temperature also drive the same stacking interactions, and Van't Hoff analysis corroborates the concentration-driven ΔG_{SA} values.[9]

The tunable twisted monomers assemble because of their unique encoding. Even more remarkably, monomers with different codes are able to assemble simultaneously and independently from a mixture. To test code specificity, we compared the concentration-dependent δ_{obs} values in a heterogeneous equimolar 1:1:1 mixture of compounds **1**, **3**, and **4** to those of the individual homogeneous solutions (Figure 1 d).[9] Remarkably, the mixture self-organizes so that

the monomers with different twist angles selectively self-assemble with identical species, and very little cross-assembly apparently occurs. If the molecular codes were interchangeable, the three independent critical self-assembly concentrations would collapse into one critical concentration and the highly twisted compound **4** would assemble at much lower concentrations than in the homogeneous case.

We have defined a new physical quantity χ_{CA} to describe the extent of cross-assembly. The dependence of χ_{CA} on the PDI code-enabling twist angles is shown in Table 1, with the difference in the homogenous and heterogeneous assembly situations particularly evident. A trace amount of compound **B** was added to a concentrated homogeneous solution of monomer **A**, and the chemical shifts of each monomer in the mixture were recorded (δ_{obs}) and compared to their chemical shifts in infinitely dilute homogeneous solutions (δ_{dil}).[9] This provides a numerical value for the extent of cross-assembly (χ_{CA}) between compounds with different twist, where $\chi_{CA} = (\delta_{B,dil} - \delta_{B,obs})/(\delta_{A,dil} - \delta_{A,obs})$. Thus, $\chi_{CA} = 1$ for indistinguishable (redundant) codes and $\chi_{CA} = 0$ for completely independent codes. These χ_{CA} values suggest that **1**, **3**, and **4** establish mostly unique molecular codes, while **2** exhibits significant cross-assembly with **1** and **3** (see Table 1). The χ_{CA} value is generally independent of the concentration of monomer **A**. Remarkably, cross-assembly is limited except for compounds with similar twist angles. A χ_{CA} value of less than 0.2 results in essentially separate codes, which corresponds to a $\Delta\theta$ value of approximately 15°. The twist angle alone, which ranges from 0 to 37°, provides at least three distinguishable codes. Therefore, molecular shapes act as selective molecular codes that control self-organization.

Table 1: Extent of cross-assembly between two compounds **A** and **B**

Compound[a]	**1**	**2**	**3**	**4**
1	1.00[b]	0.57	0.18	0.02
2	–	1.00	0.36	0.04
3	–	–	1.00	0.15
4	–	–	–	1.00

[a] Concentrated compound **A** in left column, dilute compound **B** along top row. [b] $\chi_{CA} = 1$ for indistinguishable codes (no selectivity) and $\chi_{CA} = 0$ for completely independent codes (absolute selectivity).

Phosphoramidite coupling chemistry was used to relate the value of $\Delta\theta$ to the yield of a cyclization reaction between differently twisted PDIs (Scheme 2) Different reaction yields were obtained because similarly coded molecules effectively reduce the activation entropy of coupling. Reaction of the bifunctionalized planar monomer **5** with various twisted monomers **1**–**4** in separate reactions afforded bichromophoric cyclic compounds **6**–**10**, which were isolated in all cases in addition to other linear products. However, the reaction yield of the desired binary cyclic compounds decreased as the twist angle of the starting monomers **1**–**4** increased. The yield of each reaction and data supporting the existence of molecular encoding effects during the reactions is summarized in Scheme 2.

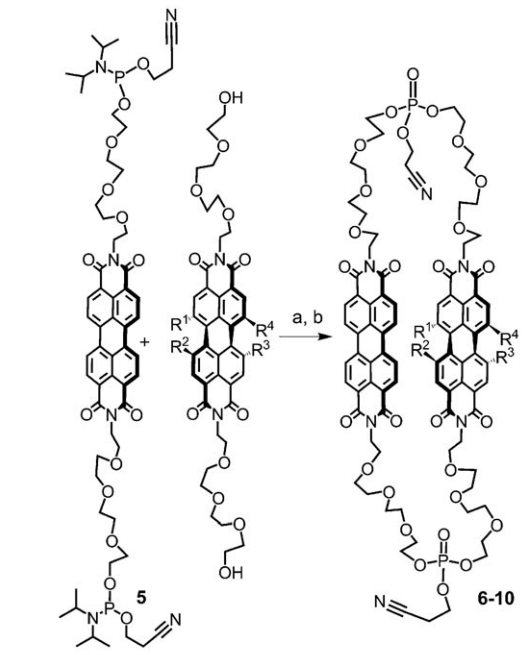

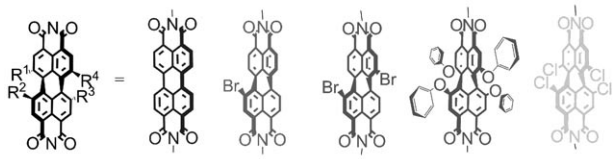

Compound	**6**	**7**	**8**	**9**	**10**
$\Delta\theta$ (deg)	0°	14°	23°	25°	37°
yield (%)	27%	27%	6%	6%	4%
$\Delta\delta$ (ppm)	0.65	0.50	0.35	0.28	0.06
r_{obs}	0.73	0.88	1.17	-	1.57

Scheme 2. The planar bisphosphoramidite **5** was treated separately with various twisted monomers to form cyclic structures **6**–**10**.[9] As the value of $\Delta\theta$ increases, reaction yields diminish because of deteriorating compatible assembly codes. Concomitantly, the upfield chemical shift ($\Delta\delta$) induced by the π stack decreases and the absorbance vibronic peak ratio (r_{obs}) increases providing reliable metrics of code compatibility. Reagents: a) CH_2Cl_2, *N*-phenylimidazolium triflate; b) 0.2 M I_2 (CH_2Cl_2/pyridine/H_2O 1:3:1).

Stronger attraction between planar precursors drives the formation of a self-assembled stack, which reduces the activation entropy for coupling and favorably orients the reaction centers for a cooperative cyclization reaction that preferentially yields cyclic products over other possible linear polymer structures. As the difference in twist angle ($\Delta\theta$) increases, the intermolecular assembly codes no longer hold and the formation of heterochromophoric cyclic compounds becomes less probable than other random collision products.

In all cases, the distance between the two cooperative reaction centers is the same, roughly 39 Å. The nanoenvironment of the reaction centers is also the same because both are bound to tetraethylene glycol linkers. Electronic effects such as electron induction or hyperconjugation from the perylene unit (through-bond effects) cannot contribute to the reactivity difference or alter the reaction course because the reaction center is approximately 14 Å away from the perylene unit. At

such an isolated position, perylene can hardly impart any steric repulsion (through-space effects). The experimental results demonstrate that molecular self-assembly invokes selective coding phenomena and the reactions follow the molecular codes programmed by the design of the PDIs.

The restrictive cyclic architectures force the chromophores into proximity irrespective of the concentration. In a similar way as the extent of homogeneous self-assembly can be calculated by UV/Vis and NMR spectroscopy, the extent of folding in covalently bound heterodimers can also be derived using these spectroscopic techniques.[9] The r_{obs} and $\Delta\delta$ values for compounds **6**–**10** are summarized in Scheme 2. Despite the restrictive architectures, cyclic dimers with incompatibly coded chromophores (**10**) are essentially unfolded, whereas compatibly coded structures (**6**) are strongly folded. Both UV/Vis and NMR spectroscopy show that molecular shapes act as codes for self-assembly.

Of course, monomers with similar twist angles tend to self-organize irrespective of the presence of other coded structures. The next natural step was to test whether such molecular codes can direct chemical reactions to form specific products. Homochromophoric exotic catenane and ring structures were previously synthesized from compounds **1** and **4** by using disulfide linkages.[14,15] From homogenous mixtures of reactive monomers, planar **11** formed monomer ring **13**, dimer ring **14**, and concatenated rings **15**, while highly twisted compound **12** only yielded homochiral or heterochiral dimer ring **16**.

To validate the molecular code concept, we employed a 1:1 heterogeneous reaction mixture of compounds **11** and **12**, which have identical reactive functional groups and can undergo the same disulfide bond formation (Scheme 3). If the reaction pathway was not driven by a molecular code, the reaction products would contain an indistinguishable statistical mixture of two building blocks **11** and **12**. Convincingly, only the homoreaction products **13**–**16**, also formed in the separate homogeneous reactions, could be isolated; no cross-assembled product such as heterogeneous ring compound **17** was detected, regardless of when the reaction was quenched. The heterogeneous reaction proceeded as if the reactions had occurred in separate flasks, thus demonstrating that the molecular codes determined by the structures with different twist angles effectively direct the reaction products. Therefore, it is self-assembly and not a random collision mechanism that dominates the reaction course.

In contrast, the heterogeneous mixture of similarly coded planar compounds **11** and **18** resulted in a new cross-assembled compound, the heterochromophoric cyclic dimer **22** (Scheme 3). NMR and UV/Vis spectroscopy demonstrate that both planar compounds independently display strong homogeneous π-stacking interactions while jointly exhibiting strong heterogeneous π-stacking interactions.[9] Even though the monosulfur compound **18** has a larger potential π-stacking area and the addition of such a five-membered ring enlarges its size and generates a slightly higher π-stacking force, the difference is not sufficient to form a unique code, thereby providing an example of code redundancy.

In summary, when two species barely interact ($\chi_{CA} = 0.02$), experimental results show their reactions proceed as if carried

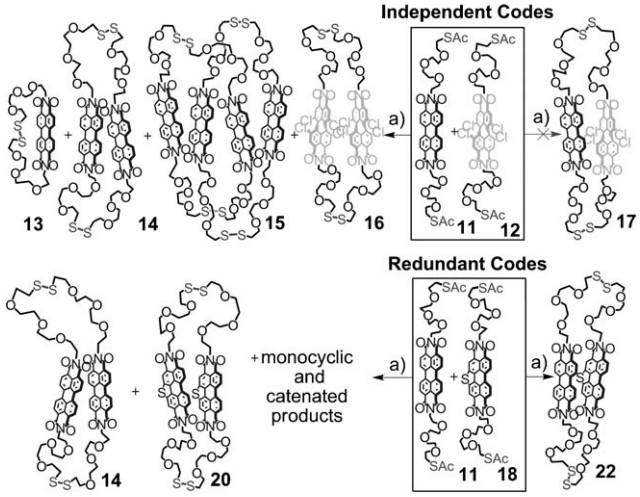

Scheme 3. Reaction between independently coded monomers **11** and **12** results in only homochromophoric products **13**–**16**, the identical products observed in homogeneous reactions in separate flasks. No heterochromophoric cyclic product **17** was isolated. However, reaction between redundantly coded planar monomers **11** and **18** resulted in new heterochromophoric compound **22**, manifesting cross-assembly between compatible codes. Conditions: a) NaOMe, CH_2Cl_2, air; H^+ quench.

out in separate flasks, with molecular codes effectively directing their distinct separate reaction pathways. When two species co-self-assemble ($\chi_{CA} \approx 1.0$), experimental results show that molecular codes become redundant and the same or very similar reaction pathways are followed. The imprinted twist-angle (structural architecture) determines the thermodynamic parameters and directs solvophobic interactions, thereby establishing useful molecular codes. The similarity limits in the twist angle for PDI code compatibility, $\Delta\theta_{twist} > 15°$, effectively distinguishes unique molecular codes, which correspond to a ΔG_{SA} value of about 1 kcal mol^{-1}. Differences in chemical shift ($\Delta\delta$) and absorbance ratio (r_{obs}) effectively report the extent of π stacking, thus providing metrics for code deciphering.

Understanding the forces that direct self-assembly represents a crucial step forward in recreating the mechanisms nature employs for efficient and specific synthesis of macromolecules. Twisting the PDI cores over a range of angles effectively tunes the π-stacking force, which imprints distinct molecular shapes and provides at least three independent codes capable of organizing reaction centers and directing separate reaction outcomes. Thus, a new hypothesis emerges: matching molecular size, shape, and charge produces synergistic weak intermolecular attractive forces, which impart molecular codes; such molecular codes effectively control chemical reaction pathways and products.

Received: June 3, 2008
Published online: September 2, 2008

Keywords: molecular recognition · perylenes · selectivity · self-assembly · supramolecular chemistry

[1] a) G. M. Whitesides, J. P. Mathias, C. T. Seto, *Science* **1991**, *254*, 1312; b) X. Li, D. R. Liu, *Angew. Chem.* **2004**, *116*, 4956 – 4979; *Angew. Chem. Int. Ed.* **2004**, *43*, 4848 – 4870; c) B. Hess, A. Mikhailov, *Science* **1994**, *264*, 223 – 224; d) T. Misteli, *J. Cell Biol.* **2001**, *155*, 181 – 185.

[2] a) S. J. Rowan, S. J. Cantrill, G. R. L. Cousins, J. K. M. Sanders, J. F. Stoddart, *Angew. Chem.* **2002**, *114*, 938 – 993; *Angew. Chem. Int. Ed.* **2002**, *41*, 898 – 952; b) P. Mukhopadhyay, P. Zavalij, L. Isaacs, *J. Am. Chem. Soc.* **2006**, *128*, 14093 – 14102.

[3] a) G. M. Whitesides, M. Boncheva, *Proc. Natl. Acad. Sci. USA* **2002**, *99*, 4769 – 4774; b) F. J. M. Hoeben, P. Jonkheijm, E. W. Meijer, A. P. H. J. Schenning, *Chem. Rev.* **2005**, *105*, 1491 – 1546.

[4] a) M. M. J. Smulders, P. H. J. Schenning, E. W. Meijer, *J. Am. Chem. Soc.* **2008**, *130*, 606 – 611; b) E. A. Meyer, R. K. Castellano, F. Diederich, *Angew. Chem.* **2003**, *115*, 1244 – 1287; *Angew. Chem. Int. Ed.* **2003**, *42*, 1210 – 1250; c) D. H. Busch, *Top. Curr. Chem.* **2005**, *249*, 1 – 65; d) G. J. Gabriel, S. Sorey, B. L. Iverson, *J. Am. Chem. Soc.* **2005**, *127*, 2637 – 2640.

[5] a) W. Su, Y. Zhang, C. Zhao, X. Li, J. Jiang, *ChemPhysChem* **2007**, *8*, 1857 – 1862; b) Z. Chen, U. Baumeister, C. Tschierske, F. Wurthner, *Chem. Eur. J.* **2007**, *13*, 450 – 465; c) M. J. Ahrens, L. E. Sinks, B. Rybtchinski, W. Liu, B. A. Jones, J. M. Giaimo, A. V. Gusev, A. J. Goshe, D. M. Tiede, M. R. Wasielewski, *J. Am. Chem. Soc.* **2004**, *126*, 8284 – 8294; d) Y. Li, Y. Li, J. Li, C. Li, X. Liu, M. Yuan, H. Liu, S. Wang, *Chem. Eur. J.* **2006**, *12*, 8378 – 8385.

[6] a) X. Zhang, Z. Chen, F. Wurthner, *J. Am. Chem. Soc.* **2007**, *129*, 4886 – 4887; b) H. Langhals, R. Ismael, O. Yuruk, *Tetrahedron* **2000**, *56*, 5435 – 5441; c) C. Kohl, T. Weil, J. Qu, K. Mullen, *Chem. Eur. J.* **2004**, *10*, 5297 – 5310.

[7] a) W. Wang, J. J. Han, L.-Q. Wang, L.-S. Li, W. Shaw, A. D. Q. Li, *Nano Lett.* **2003**, *3*, 455 – 458; b) W. Wang, L.-S. Li, G. Helms, H. Zhou, A. D. Q. Li, *J. Am. Chem. Soc.* **2003**, *125*, 1120 – 1121.

[8] a) F. Würthner, *Chem. Commun.* **2004**, 1564 – 1579; b) P. Osswald, F. Wurthner, *J. Am. Chem. Soc.* **2007**, *129*, 14319 – 14326; c) W. Wang, A. D. Bain, L.-Q. Wang, G. J. Exarhos, A. D. Q. Li, *J. Phys. Chem. A* **2008**, *112*, 3094 – 3103.

[9] See the Supporting Information for complete experimental details, synthesis, and characterization of compounds **2**–**3**, **5**–**10**, and **18**–**22**, and additional supporting figures and tables.

[10] A. D. Q. Li, W. Wang, L. Q. Wang, *Chem. Eur. J.* **2003**, *9*, 4594 – 4601.

[11] $r_{obs} \approx$ Huang–Rhys factor^{-1}.

[12] F. C. Spano, S. C. J. Meskers, E. Hennebicq, D. Beljonne, *J. Am. Chem. Soc.* **2007**, *129*, 7044 – 7054.

[13] R. B. Martin, *Chem. Rev.* **1996**, *96*, 3043 – 3064.

[14] W. Wang, L. Q. Wang, J. Palmer, G. Exarhos, A. D. Q. Li, *J. Am. Chem. Soc.* **2006**, *128*, 11150 – 11159.

[15] W. Wang, A. D. Shaller, A. D. Q. Li, *J. Am. Chem. Soc.* **2008**, *130*, 8271 – 8279.